Progress In Electromagnetics Research C, Vol. 124, 43–52, 2022

A Compact Ultra-Wide Band Printed Log-Periodic Antenna Using a Bow-Tie Structure

Massimo Donelli[1, *], Mohammedhusen Manekiya[1], Viviana Mulloni[2], Giada Marchi[2], and Roberto Mendicino[2]

Abstract—This letter, an ultra-wideband compact printed log periodic dipole (LPD) array antenna is designed to operate between 500 MHz and 6 GHz frequencies. The proposed LPD antenna structure consists of one bow-tie dipole and 15 regular dipole elements. The bow-tie element is introduced to improve the antenna's performance at the lowest frequencies below 1 GHz and at the same time to reduce the antenna size maintaining a good performance. An experimental antenna prototype has been designed, optimized, fabricated, numerically and experimentally assessed. The obtained results are very promising, and they demonstrated that the presented antenna prototype is able to operate in the range between 500 MHz and 6 GHz with an average gain of 6 dBi and a very compact size.

1. INTRODUCTION

In the last years, the rapid evolution of radio communication techniques able to transmit information over a large portion of the radio spectrum at very low energy levels required the development of high efficient high bandwidth antennas. An ultra-wideband (UWB) radiating device must accomplish the legislation provided by the Federal Communications Commission (FCC) and European Communication Committee (ECC) [1]. UWB antennas working at high frequencies present high propagation losses with respect to low-frequency bands, so high gain and wideband antennas are required to mitigate the losses in high-frequency ranges. Microstrip technology permits the development of a compact, light weight antenna that can provide UWB characteristics with high performance in terms of radiation properties. Radiofrequency identification (RFID) systems operating in the ultra-high frequency (UHF, 860–960 MHz) provide higher read-rate and data rate than those in low frequency (LF, 119–135 kHz) and high frequency (HF, 13.56 MHz) [2]. However, in UHF band, the selective loop is comparable to the operating wavelength. Out-of-phase currents appear on the loop, which leads to nonuniform and rapid magnetic field variation in the near-field range. Wideband antennas have various applications in many fields, such as localization of the unknown signal source to track, radar imaging systems, sensors, and surveillance. The current communication data transmission systems are based on short pulses. The Federal Communications Commission (FCC) has restricted short pulse power; thus, communication is limited to a 10 m range in indoor environments. A well-known and diffuse wideband end-fire antenna is a log periodic dipole (LPD) antenna, which is very famous thanks to its good radiating properties. In particular, printed log-periodic dipole array antennas have light weight, low cost, and high gain. Moreover, they present good directivity and wide bandwidth. The main limitations of UWB systems are narrowband pulse dispersion and low fidelity factor that affect the antenna's parameters. To improve the performance of LPD antennas, several design structures have been proposed, such as sinusoidal curve [3], T-shape slot dipole [4], printed Log-Yagi dipole array antenna (PLYDA) [5], passive-interface

Received 3 July 2022, Accepted 14 August 2022, Scheduled 12 September 2022

* Corresponding author: Massimo Donelli (massimo.donelli@unitn.it).

[1] Department of Environmental and Mechanical Engineering, University of Trento, 38100, Italy. [2] Center for Materials and Microsystems (CMM), Fondazione Bruno Kessler (FBK), 38123, Italy.

circuit module [6], square fractal antenna [7], dual-band dipole element [8], half bow-tie printed dipole antenna [9], bow-tie patch [10], and top-loading technique [11]. A miniaturized LPD antenna with a sinusoidal shaped dipole is proposed for wideband application in [3]. The antenna size is miniaturized with a width of 420 mm (0.28λ) using dielectric-loaded and sinusoidal-shaped dipoles. The optimized antenna has a bandwidth of 200–800 MHz and gain of 4.5 dBi. In [4], T-shape slot dipoles are arranged in the array of 12 elements, in which 6 elements are for horizontal polarization and 6 for vertical polarization. T-slits reduce the mutual coupling between the vertical and horizontal elements. The printed log-periodic dipole (PLPD) array antenna using a director cell presented in [5] is designed for 21–40 GHz. A time-reversal UWB optimization technique is proposed in [6] to improve the fidelity factor and radiated peak signal. In [8], a dual-band dipole element based printed LPD antenna is proposed for an operating frequency of 0.5–10 GHz. A dual-band dipole replaces the need for two straight dipoles; therefore, the axial length of the LPD antenna is reduced. The structured shape, like a square, printed bow-tie, or bow-tie patch, explicitly reduces the antenna's size and improves the performance compared to other structures. In [7], a fractal geometry-based multi-band antenna is proposed. The formation of fractal reduces the size of the element by 23%. Similarly, in [9] and [10] a bow-tie based balun dipole element and a bow-tie patch element are proposed, respectively. The balun shape dipole element provides wide impedance bandwidth of 47% for the 2.4 GHz ISM band, whereas the bow-tie patch provides 60% impedance bandwidth with low cross-polar radiation 7 dBi gain in the ISM band. To further reduce the size of the bow-tie antenna element and improve the radiation characteristics of the overall antenna, double-sided round bow-tie [12], sweeping the radiating slots in a circular manner [13], and an asymmetric coplanar waveguide [14] have been presented. Research like [15–17] mainly focuses on a frequency reconfigurable bow-tie antenna for Bluetooth, WiMAX, and WLAN applications. In [15, 17], reconfiguration is achieved by employing p-i-n diodes over the bow-tie arms, changing the effective electrical length of the antenna, and leading to an electrically tunable operating band. In comparison, [16] demonstrated a triple band slotted bow-tie monopole. A printed bow-tie structure has an application in UWB, Ku/K/Ka bands, and millimeter-wave imaging [18]. In [19], a flexible bow-tie antenna has been presented with a detailed explanation of design and fabrication. In addition, the radiation characteristics of antennas, effects of the feeding structure, and conductor losses on the radiation performance of the antenna have been discussed. The examination of bow-tie curvature impact on the radiation pattern has been done in detail. This paper proposes a miniaturized microstrip LPD array antenna for UWB applications. In particular, a bow-tie structure, consisting of two antipodal empty triangular segments, operating at low frequencies, has been introduced to reduce the antenna size and at the same time to improve the antenna performance. An antenna prototype has been designed, optimized, fabricated, numerically and experimentally assessed. The agreement between simulated and measured results is quite good. The antenna performances are very promising; they present a bandwidth B of 0.5–6 GHz, peak radiation efficiency of 98%, and peak gain of 6.2 dBi in the operating frequency band. The obtained promising results of the LPD antenna make it particularly suitable for several high-speed short distance communication applications, including surveillance, explosive detection, sensing, and security scanning. The work is organized as follows. Section 2 reports the mathematical formulation and related design methodology. Section 3 reports the numerical and experimental assessment. Finally, Section 4 reports the conclusions.

2. ANTENNA DESIGN

The structure of a UWB log-periodic printed antenna and the proposed prototype equipped with a bow-tie structure is shown in Figures 1(a) and (b), respectively.

A classical printed LPD antenna, reported in Figure 1(a), is composed of a set of dipole elements printed on both sides of the substrate to obtain an antipodal feeding network structure. The resonance frequency of every antenna element changes periodically, considering a logarithmic function related to the frequency. In particular, with reference to Figure 1(a) and considering N dipole elements, the following set of geometrical parameters must be properly tuned to obtain a working antenna, $P_{\text{standard}} = \{L_n, D_n, n = 0, ..., N-1, W_s, W_0, L_{\text{stub}}\}$ where L_n and D_n are the lengths and inter elements distance of the dipoles; W_s is the microstrip width of the dipoles; W_0 is the width of feeding microstrip; and L_{stub} is the length of a stub aimed at the antenna impedance matching. The design procedure of a

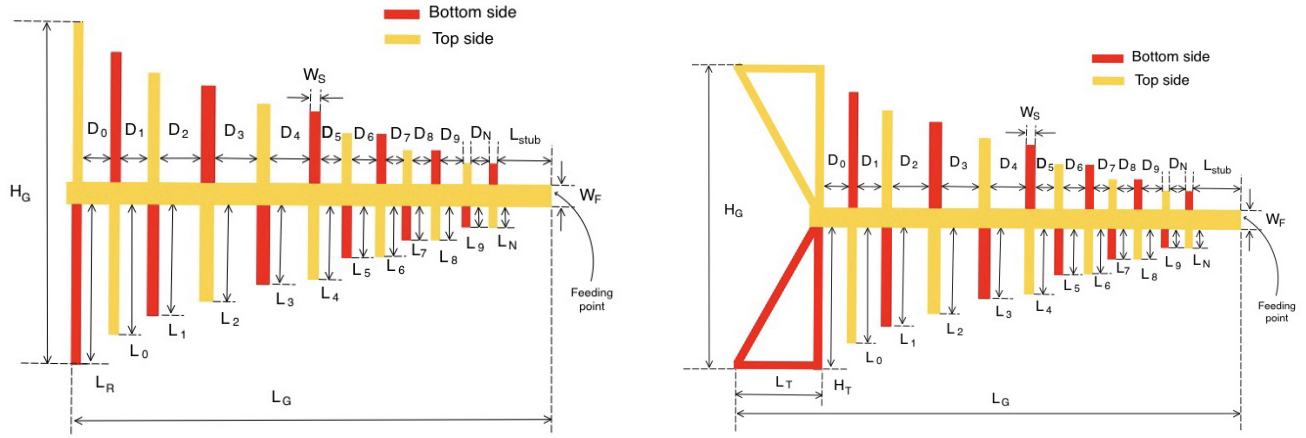

Figure 1. Structure and geometrical parameter of (a) standard LPD antenna, (b) LPD antenna equipped with the bow-tie structure.

printed LPD antenna is summarized in [22]. The starting point is the definition of antenna requirements in terms of bandwidth by fixing the minimum $f_{\min}$ and maximum $f_{\max}$ frequencies. The relative operating bandwidth B is defined as the ratio between the highest and lowest working frequencies of the LPD antenna:

$$B = \frac{f_{\max}}{f_{\min}} \tag{1}$$

by considering the antenna dimensions L_G and $H = 2L_R$ the angle α is estimated by using the following relation:

$$\alpha = a\tan\left(\frac{L_G}{2H}\right) \tag{2}$$

The angle α and scaling parameter τ, which can be chosen considering the empirical rules reported in [20, 21], allow us to compute the total number of dipole elements N as follows:

$$N = 1 + \frac{\log\left(B_s \cdot (1.1 + 7.7(1-\tau^2)\cot(\alpha))\right)}{\log\left(1/\tau\right)} \tag{3}$$

The two most important antenna design parameters are the ratio between length of two consecutive dipoles L_n and L_{n+1} known as the scaling factor τ, and the spacing between elements σ. The optimal relative inter-element distance σ_{op}, which relates the spacings with dipoles length, is given by [20, 21]:

$$\sigma_{opt} = 0.243 \cdot \tau - 0.051 = \frac{D_n}{L_n} \tag{4}$$

The ratio between distances of two consecutive dipoles $\sigma = L_n/L_{n-1}$, $n = 1, \ldots, N$, and the ratio between the distance of an arm and the spacing from next one is related to the scaling factor τ as follows, $\tau = D_n/L_n$, $n = 1, \ldots, N$.

The arms impedance is the ratio between arm's length L_n and arm's width W_n. Given that the exponential trend that these two parameters are the same, this ratio is constant for all antenna elements. Following [20] the average arm width that permits setting the characteristic impedance Z_0 is given by:

$$W_n = \frac{L_n}{e^{2.25+\frac{Z_0}{120}}} \tag{5}$$

The last remaining geometrical parameters to set are the arm width, W_s, main feeding microstrip width W_0, and stub length L_{stub} aimed at tuning the antenna impedance. The above semi-empirical formulas (1)–(5) provide a guideline for the design of a standard printed LPD antenna. The performances and dimensions of a standard LPD antenna are not so satisfactory especially at low frequencies. Modern

telecommunication systems require very compact antennas, so the goal of a new antenna design is to improve antenna performances in terms of return loss S_{11} especially at low frequency, to further reduce the antenna dimension with respect to standard design, and finally to obtain a flatter behaviour in terms of return loss S_{11} and gain versus frequency. The main problem is the dimension reduction especially at low frequency. To obtain a more compact design, different techniques can be used, such as the use of high dielectric permittivity substrate or the use of fractal geometries. Both methodologies are very effective, but the use of high dielectric permittivity substrates is quite expensive, while the use of fractal geometries does not permit the proper control of resonances. The solution proposed for this design considers an empty triangular bow-tie structure able to resonate at low frequencies and provide a very compact structure with respect to the standard design and the other methodologies presented in scientific literature. With the knowledge of authors the obtained antenna design is the most compact with respect to the other prototypes presented in scientific literature. To properly design and tune the antenna geometrical parameters reported in Figure 1(b), a tuning phase provided by a suitable optimization tool has been considered. However, a final tuning phase provided with a suitable optimization tool is mandatory to accomplish the antenna requirements.

3. NUMERICAL AND EXPERIMENTAL RESULTS

The following subsections present the antenna prototype design, numerical and experimental assessment. The obtained results are commented on and discussed.

3.1. Numerical Assessment

Let us start with the design of a standard LPD printed antenna on a commercial dielectric substrate, namely Arlon25N ($\varepsilon_r = 3.38$, $\tan(\delta) = 0.03$, thickness $t = 0.8\,\text{mm}$). The antenna requirements are $f_{\min} = 0.5\,\text{GHz}$, $f_{\max} = 6\,\text{GHz}$, antenna impedance $Z_0 = 50\,\Omega$. The first step is the preliminary choice of the scaling factor τ and the relative spacing σ that can be made from the normalized graph reported in [20]. The determination of boom length L_g and number of elements N are provided by relations (2) and (3), respectively. In particular, considering the required bandwidth of $B = f_{\max}/f_{\min} = 12.0$ a number of $N = 12$ dipole elements are obtained. The most extended dipole L_R corresponds to the lowest resonance frequency, and it can be computed by considering the following equation

$$L_R \approx \frac{\lambda_{eff\,\max}}{4} = \frac{c}{\sqrt{\varepsilon_{eff}}\, f_{\min}} \tag{6}$$

where ϵ_{eff} is the effective dielectric permittivity; ϵ_r and h are relative permittivity and height of the substrate; and w is the width of antenna element. The length L_n and spacing D_n of the others elements are estimated by considering the ratio between distances of two consecutive dipoles $\sigma = L_n/L_{n-1}$, $n = 1, \ldots, N$, and $\tau = D_n/L_n$, $n = 1, \ldots, N$. For the proposed $N = 12$ elements LPD antenna with an operating frequency of 0.5–6 GHz the other design parameters are provided in Table 1. The antenna has been numerically assessed with the Advanced Design System (ADS) from Keysight Company. The geometrical parameters reported in Table 1 have been optimized by using the optimization tool of ADS software in order to maximize the antenna performances.

Concerning the last two geometrical parameters, namely the width of the main feeding stripline $W_f = 2.0\,\text{mm}$ and the stub length $L_{\text{stub}} = 7.0\,\text{mm}$. In order to improve the antenna performances, the longest dipole of LPDA has been replaced with a printed bow-tie structure, which is similar to the design of rectangular microstrip patches. The bow-tie geometrical parameters are estimated by modifying the semi-empirical design relations for rectangular patches given in [22]. Then the final antenna geometrical parameters are fine-tuned and finalized via numerical simulations and the optimization tool of the ADS software. In particular, the bow-tie structure presents the following geometrical dimensions $L_T = 29.5\,\text{mm}$ and $H_G = 90.0\,\text{mm}$. The overall dimension of the standard LPD antenna structure is $66 \times 95\,\text{mm}^2$, while the dimension of LPD antenna equipped with the bow-tie structure is $91 \times 95\,\text{mm}^2$. The simulated return loss obtained with the ADS structure in the whole considered frequency band is reported in Figure 2 for standard and bow-tie LPD antenna. As can be noticed, the introduction of the bow-tie element slightly increases the antenna length. The introduction of the bow-tie structure produces an improvement of the return loss (S_{11}) at low frequency, as reported in Figure 2.

Table 1. Geometrical design parameters of proposed printed LPD antenna.

Dipoles (n)	Length of dipoles (L_n) in mm	Width of dipoles (W_n) in mm	Spacings (D_n) in mm
0	$L_R = 44.5$	$W_0 = 2.8$	$D_0 = 7.5$
1	$L_0 = 38.0$	$W_1 = 2.7$	$D_1 = 6.0$
2	$L_1 = 32.0$	$W_2 = 2.3$	$D_2 = 5.0$
3	$L_2 = 27.0$	$W_3 = 2.2$	$D_3 = 4.5$
4	$L_3 = 23.0$	$W_4 = 1.9$	$D_4 = 3.9$
5	$L_4 = 19.0$	$W_5 = 1.8$	$D_5 = 3.1$
6	$L_5 = 16.0$	$W_6 = 1.7$	$D_6 = 2.8$
7	$L_6 = 14.0$	$W_7 = 1.7$	$D_7 = 2.0$
8	$L_7 = 12.0$	$W_8 = 1.6$	$D_8 = 1.9$
9	$L_8 = 10.5$	$W_9 = 1.5$	$D_9 = 1.6$
10	$L_9 = 9.0$	$W_{10} = 1.4$	$D_{10} = 1.1$
11	$L_{10} = 7.5$	$W_{11} = 1.3$	
12	$L_{11} = 6.5$		

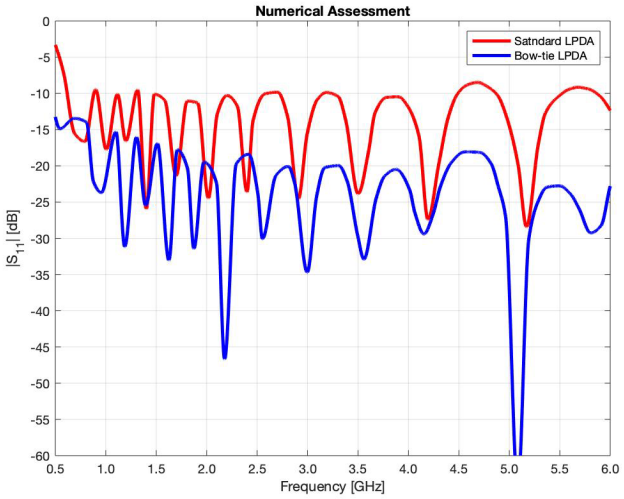

Figure 2. Numerical assessment, return loss (a) (red-line) standard LPD antenna, (b) (blue-line) LPD antenna equipped with the empty bow-tie triangular structure.

3.2. Experimental Assessment

The geometrical parameters estimated in the previous subsection are used to fabricate two antenna prototypes, a standard antenna and the proposed LPD antenna. The two prototypes have been printed on a commercial dielectric substrate ARLON 25N ($\varepsilon_r = 3.38$, $t = 0.8\,\text{mm}$, and $\tan(\delta) = 0.001$) with a computer numeric control machine and equipped with a subminiature type A (SMA) coaxial connector. The photos of antenna prototypes are reported in Figures 3(a) and (b), respectively. The antenna prototypes have been arranged inside a semi-anechoic chamber, and the return loss $|S_{11}|$ has been measured with a network analyzer (NA). The results are reported in Figure 4. As can be noticed from the data reported in Figure 4, the bow-tie antenna outperforms a standard LPD antenna, and the return loss is well below $|S_{11}| < -10\,\text{dB}$ for almost the entire considered frequency band. For the sake

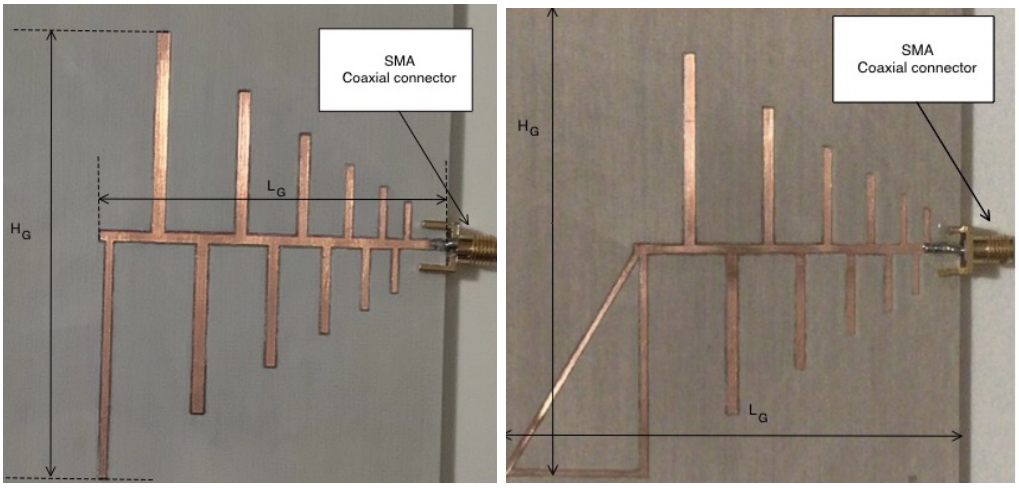

(a) (b)

Figure 3. Photographs of the two antenna prototypes (a) standard LPD antenna, (b) LPD antenna equipped with the bow-tie structure.

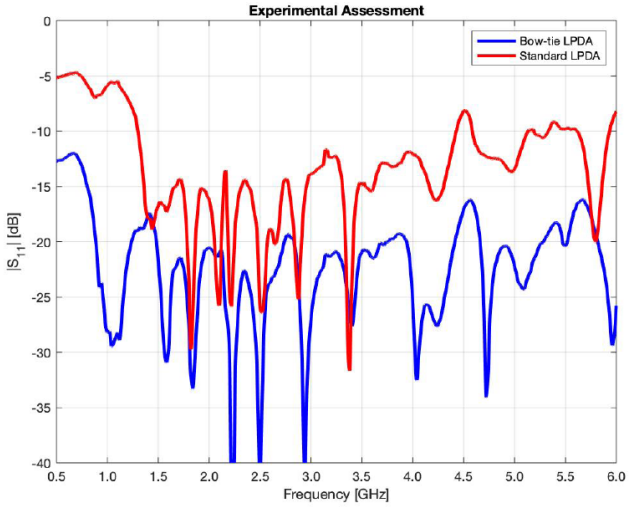

Figure 4. Comparison of experimental and numerical return losses for the standard and bow-tie LPD antennas.

of completeness in Figures 5(a) and (b), the measured and numerical return losses are compared for the standard and bow-tie LPD antenna. The agreement between numerical and measured data is not perfect but still satisfactory. The gain of two prototypes has been measured using three antennas to complete the antenna characterization. The results are reported in Figure 6; also, in this case, the bow-tie antenna outperforms the standard LPD antenna about 3 dBi in the whole considered frequency band. In particular, the gain versus frequency, related to the standard printed LPD antenna design, reported in Figure 4 (red line) reports a slightly low gain with respect to the theoretical value that should be about 6.5 dBi. Figure 4 (red line) presents a gain about 5.0 dBi and different strong fluctuations of the antenna gain vs. the frequency. As reported above, the gain versus frequency obtained with the proposed LPD bow-tie antenna design outperforms the standard design of 1.5 dBi reaching the theoretical value of a gain about 6.5 dBi. Moreover, the data reported in Figure 4 (blue line) related to the new design show a very flat behaviour in the whole considered frequency range. The numerical data obtained

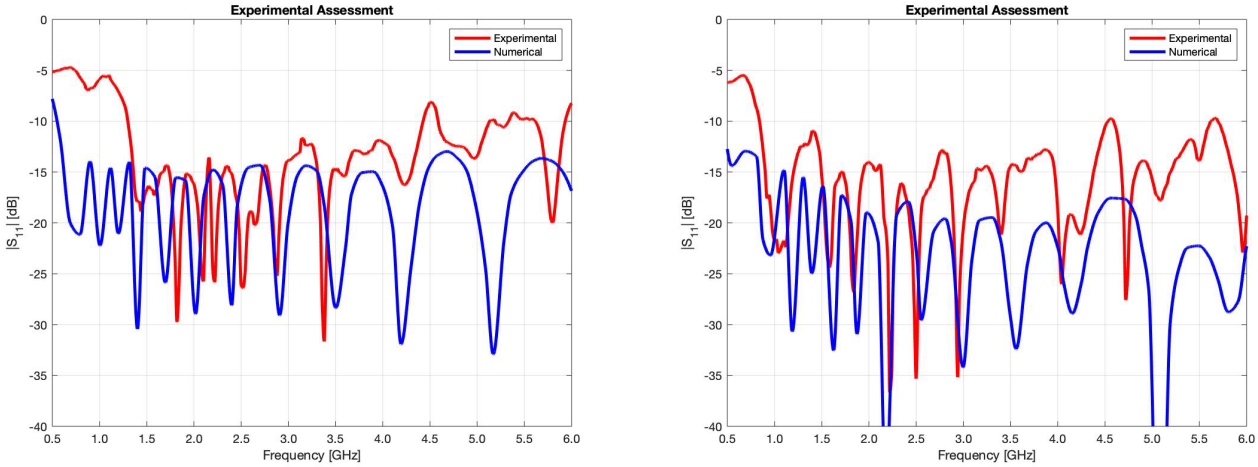

Figure 5. Comparison of experimental and numerical return losses for the bow-tie LPD antenna.

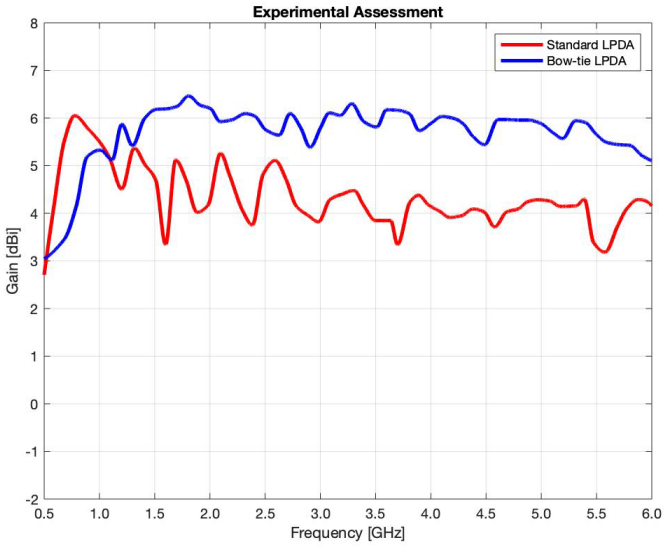

Figure 6. Experimental assessment, measured gain (a) standard LPD antenna, (b) LPD antenna equipped with the bow-tie structure.

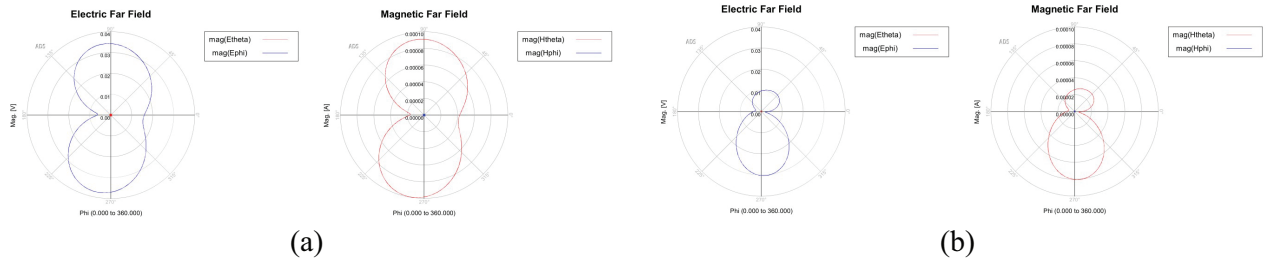

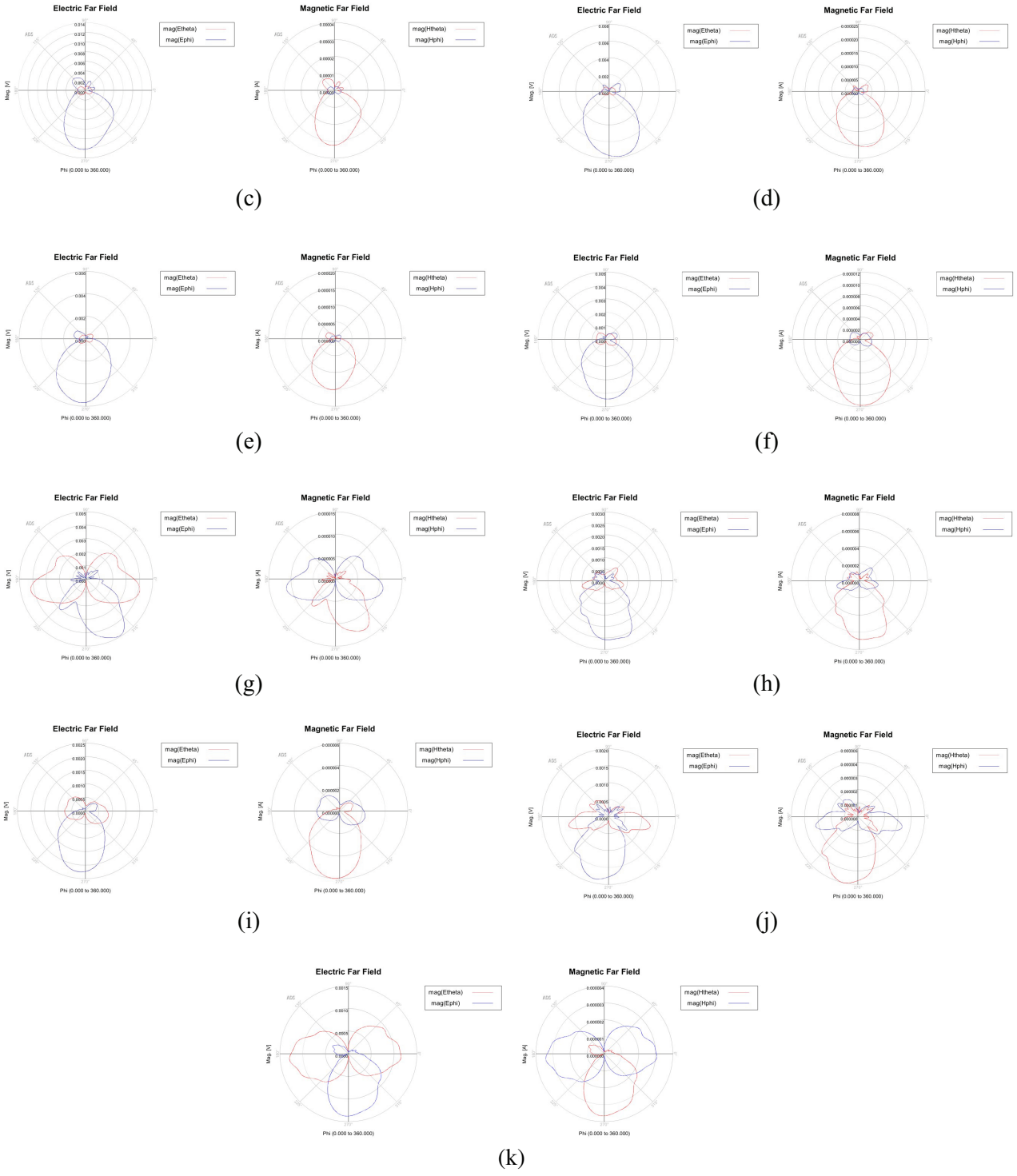

Figure 7. *E*-plane and *H*-plane beam pattern estimated for the whole considered frequency band form 500 MHz to 6 GHz with step of 500 MHz. (a) Electric and magnetic far field pattern at 500 MHz. (b) Electric and magnetic far field pattern at 1 GHz. (c) Electric and magnetic far field pattern at 2 GHz. (d) Electric and magnetic far field pattern at 2.5 GHz. (e) Electric and magnetic far field pattern at 3 GHz. (f) Electric and magnetic far field pattern at 3.5 GHz. (g) Electric and magnetic far field pattern at 4 GHz. (h) Electric and magnetic far field pattern at 4.5 GHz. (i) Electric and magnetic far field pattern at 5 GHz. (j) Electric and magnetic far field pattern at 5.5 GHz. (k) Electric and magnetic far field pattern at 6 GHz.

with a commercial software have also been compared with experimental measurements obtained with the method of three antennas in a semi-anechoic chamber. The agreement between numerical and experimental results is quite good with a discrepancy less than 5%.

For the sake of completeness, the E and H plane far field beam patterns for bow-tie LPD antenna are presented in Figures 7(a)–(k). The considered starting and stop frequencies are 500 MHz and 6 GHz, respectively, with a step of 500 MHz. The beam patterns have been firstly numerically obtained with ADS commercial simulator (Keysight company), then the beam pattern has been experimentally assessed in the semi-anechoic chamber kindly provided by the company EMC (srl), Genoa, Italy, confirming the numerically obtained data. As can be noticed from the data reported in Figure 7, the directive antenna behaviour due to the arms and empty bow-tie structure is well defined especially in the range between 2.0 and 3.5 GHz as indicated in Figures 7(c), (d), (e), and (f). The beam pattern and gain of the proposed LPD antenna equipped with the empty bow-tie structure outperform the performances obtained with standard design LPD antenna in the whole considered frequency range.

4. CONCLUSION

This work proposes a printed LPD antenna equipped with a bow-tie structure to improve the radiation characteristics at a low-frequency band. The antenna parameters have been first obtained following semi-analytic formulas and then optimized with the ADS optimization tool. An antenna prototype has been designed, optimized, fabricated, and experimentally assessed. The obtained results have been compared with a standard LPD antenna, and they are rather promising.

REFERENCES

1. "Revision of Part 15 of the commission's rules regarding ultra-wideband transmission systems," Federal Communications Commission, Dec. 15, 2015, https://www.fcc.gov/document/revision-part-15-commissions-rules-regarding-ultra-wideband (accessed Feb. 02, 2022).
2. Finkenzeller, K., *RFID Handbook: Fundamentals and Applications in Contactless Smart Cards, Radio Frequency Identification and Near-field Communication*, John Wiley & Sons, Ltd, Chichester, UK, 2010, doi: 10.1002/9780470665121.
3. Chang, L., S. He, J. Q. Zhang, and D. Li, "A compact dielectric-loaded Log-Periodic Dipole Array (LPDA) antenna," *IEEE Antennas and Wireless Propagation Letters*, Vol. 16, 2759–2762, 2017.
4. Liang, J.-J., J.-S. Hong, J.-B. Zhao, and W. Wu, "Dual-band dual-polarized compact log-periodic dipole array for MIMO WLAN applications," *IEEE Antennas and Wireless Propagation Letters*, Vol. 14, 751–754, 2015.
5. Zhai, G., Y. Cheng, Q. Yin, S. Zhu, and J. Gao, "Gain enhancement of printed log-periodic dipole array antenna using director cell," *IEEE Transactions on Antennas and Propagation*, Vol. 62, No. 11, 5915–5919, Nov. 2014, doi: 10.1109/TAP.2014.2355851.
6. Khaleghi, A., H. S. Farahani, and I. Balasingham, "Impulse radiating log-periodic dipole array antenna using time-reversal technique," *IEEE Antennas and Wireless Propagation Letters*, Vol. 10, 967–970, 2011.
7. Amini, A., H. Oraizi, and M. A. Chaychi Zadeh, "Miniaturized UWB log-periodic square fractal antenna," *IEEE Antennas and Wireless Propagation Letters*, Vol. 14, 1322–1325, 2015, doi: 10.1109/LAWP.2015.2411712.
8. Anim, K. and Y.-B. Jung, "Shortened log-periodic dipole antenna using printed dual-band dipole elements," *IEEE Transactions on Antennas and Propagation*, Vol. 66, No. 12, 6762–6771, Dec. 2018.
9. Yeoh, W. S., K. L. Wong, and W. S. T. Rowe, "Wideband miniaturized half bow-tie printed dipole antenna with integrated balun for wireless applications," *IEEE Transactions on Antennas and Propagation*, Vol. 59, No. 1, 339–342, 2011.
10. Wong, H., K. M. Mak, and K. M. Luk, "Wideband shorted bow-tie patch antenna with electric dipole," *IEEE Transactions on Antennas and Propagation*, Vol. 56, No. 7, 2098–2101, 2008.

11. Kyei, A., D. U. Sim, and Y. B. Jung, "Compact log-periodic dipole array antenna with bandwidth-enhancement techniques for the low frequency band," *IET Microwaves, Antennas & Propagation*, Vol. 11, No. 5, 711–717, 2017.
12. Karacolak, T. and E. Topsakal, "A Double-Sided Rounded Bow-Tie Antenna (DSRBA) for UWB communication," *IEEE Antennas and Wireless Propagation Letters*, Vol. 5, 446–449, 2006.
13. Berge, L. A., M. T. Reich, and B. D. Braaten, "A compact dual-band bow-tie slot antenna for 900-MHz and 2400-MHz ISM bands," *IEEE Antennas and Wireless Propagation Letters*, Vol. 10, 1385–1388, 2011.
14. Xu, L., L. Li, and W. Zhang, "Study and design of broadband bow-tie slot antenna fed with asymmetric CPW," *IEEE Transactions on Antennas and Propagation*, Vol. 63, No. 2, 760–765, Feb. 2015.
15. Li, T., H. Zhai, X. Wang, L. Li, and C. Liang, "Frequency-reconfigurable bow-tie antenna for Bluetooth, WiMAX, and WLAN applications," *IEEE Antennas and Wireless Propagation Letters*, Vol. 14, 171–174, 2015.
16. Wu, M.-T. and M.-L. Chuang, "Multibroadband slotted bow-tie monopole antenna," *IEEE Antennas and Wireless Propagation Letters*, Vol. 14, 887–890, 2015.
17. Li, T., H. Zhai, L. Li, and C. Liang, "Frequency-reconfigurable bow-tie antenna with a wide tuning range," *IEEE Antennas and Wireless Propagation Letters*, Vol. 13, 1549–1552, 2014.
18. Yurduseven, O., D. Smith, and M. Elsdon, "Printed slot loaded bow-tie antenna with super wideband radiation characteristics for imaging applications," *IEEE Transactions on Antennas and Propagation*, Vol. 61, No. 12, 6206–6210, Dec. 2013.
19. Durgun, A. C., C. A. Balanis, C. R. Birtcher, and D. R. Allee, "Design, simulation, fabrication and testing of flexible bow-tie antennas," *IEEE Transactions on Antennas and Propagation*, Vol. 59, No. 12, 4425–4435, Dec. 2011.
20. Carrel, R., "The design of log-periodic dipole antennas," *1958 IRE International Convention Record*, 61–75, 1961, doi: 10.1109/IRECON.1961.1151016.
21. Kakkar, R. and G. Kumar, "Stagger tuned microstrip log-periodic antenna," *IEEE Antennas and Propagation Society International Symposium. 1996 Digest*, Vol. 2, 1262–1265, 1996, doi: 10.1109/APS.1996.549826.
22. Balanis, C. A., *Antenna Theory: Analysis and Design*, 3rd Edition, Wiley, 1982.